CERN-TH/2001-195
hep-ph/0107247

Neutrino deep-inelastic scattering: new experimental and theoretical results

A. L. Kataev
Theoretical Physics Division, CERN CH-1211 Geneva, Switzerland and Institute for Nuclear Research of the Academy of Sciences of Russia, 117312, Moscow, Russia

Abstract

A review of recent experimental and theoretical studies of characteristics of neutrino deep-inelastic scattering is presented. Special attention is paid to the determination of α_s and $1/Q^2$ non-perturbative effects from the QCD fits to xF_3 data at different orders of perturbation theory, with the help of several theoretical methods.

Contributed to the Proceedings of Les Rencontres de la Vallée d'Aoste, La Thuile, Italy, March 4-10, 2001

CERN-TH/2001-195
July 2001

1 Introduction

The neutrino deep-inelastic scattering (DIS) is continuing to serve as the classical tool for probing the nucleon structure (for reviews, see e.g. Refs. [1] [2]). In the last few years some progress was made in more detailed experimental and theoretical studies of the behaviour of the cross-sections of νN DIS, and in the extraction of the structure functions (SFs) xF_3 and F_2. Among the data that are currently under active analysis are the ones provided by the CCFR/NuTeV collaboration at the Fermilab Tevatron (see e.g. Refs. [3] [4]), the experimental results of theJINR–IHEP Neutrino Detector collaboration [5] collected some time ago at the IHEP (Protvino) U-70 proton synchrotron, and the preliminary data of the CHORUS collaboration, obtained recently at the CERN SPS [6] [7].

The kinematical regions currently available for cross-section measurements are shown on the plot of Fig. 1, taken from Ref. [8]. This figure clearly shows that the above-mentioned three experiments were performed in different kinematical regions, which overlap in part only. Thus they provide complementary information about the behaviour of SFs in different regimes. Moreover, additional more precise data for νN DIS cross-sections can be obtained in the future at neutrino factories. If the energy of the neutrino beam is fixed at $E_\nu = 50$ GeV, experiments should penetrate into the physical region that was added to Fig.1 in Ref. [9]. This region overlaps in part with those where the above-mentioned three experimental collaborations were working. Therefore, the studies of the data on νN DIS characteristics available at present can be important milestones in the planning of more precise DIS experiments at neutrino factories [10].

2 Discussions of some new experimental results

Recent interesting experimental news came from the model-independent re-extraction of the behaviour of the F_2 νN SF [4] from the CCFR'97 data [3]. The re-analysis of Ref. [4], which does not affect previous CCFR'97 xF_3 results, removed the widely discussed discrepancy that existed at $x < 0.1$ between the behaviour of CCFR'97 F_2 [3] and that obtained by the NMC collaboration [11] from the process of μN DIS. In addition to the new extraction of F_2 from the differential cross-sections of CCFR, the first measurement of $\Delta xF_3 = xF_3^\nu - xF_3^{\overline{\nu}}$ was also performed [4]. However, it is important to stress that none of the considered non-perturbative, perturbative, and theoretical effects, including charm production, are still unable to describe the experimental results obtained for ΔxF_3 [12].

The information about the corrected behaviour of CCFR F_2 may be really important for the continuation of the work of the CHORUS collaboration. Indeed, in the kinematical region where both sets of νN DIS data overlap, the preliminary CHORUS results for xF_3 and F_2 [7] agree with the ones provided by the CCFR

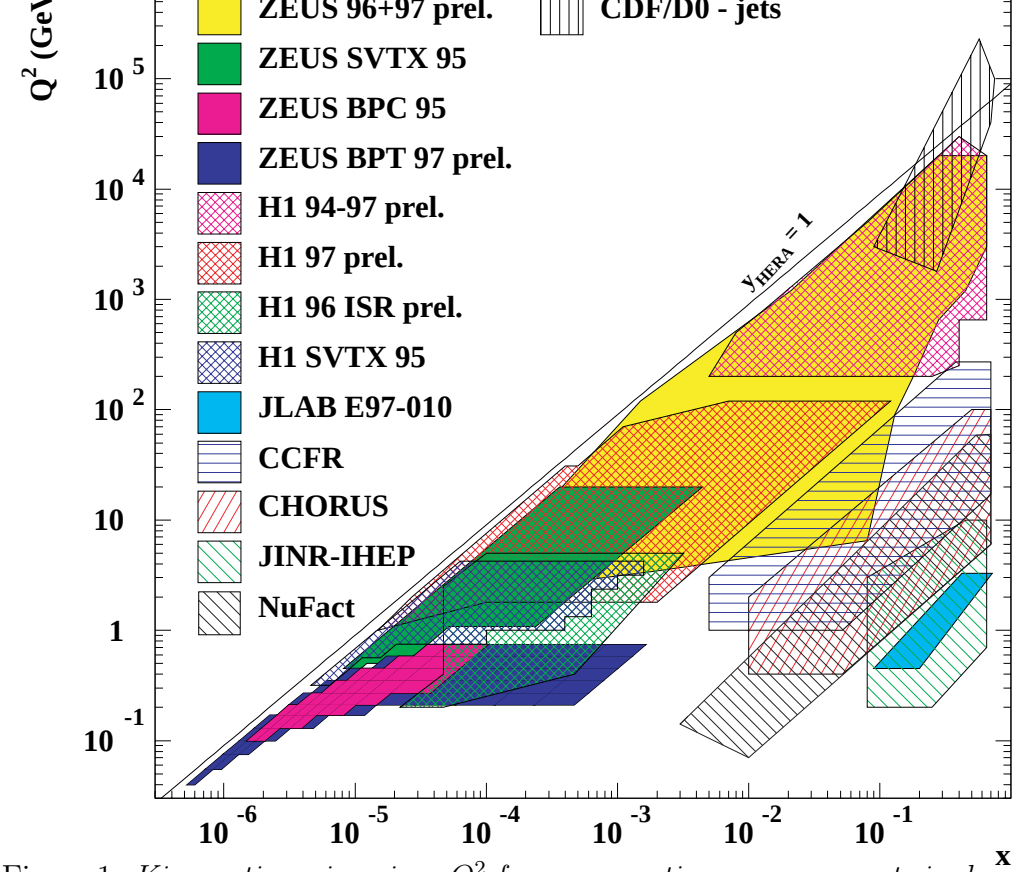

Figure 1: *Kinematic regions in x-Q^2 for cross-section measurements in deep inelastic ep scattering, ν scattering and for triple differential jet cross-section measurements in $p\bar{p}$ collisions (from Ref.* [9]*).*

collaboration in 1997 [3]. Therefore, the preliminary CHORUS F_2 data should show a pattern identical to that found in the CCFR'97 analysis [3], i.e. exceeding by 10–15% F_2 NMC measurements at $x < 0.1$. This excess is beyond the existing statistical and systematic errors of discussed DIS experiments. Moreover, the inclusion of these wrong CCFR'97 F_2 points into the next-to-leading order (NLO) QCD fits, performed with the help of the DGLAP method [13], leads to the erroneous low-x behaviour of the gluon distribution $xG(x, 9\ \mathrm{GeV}^2) \sim x^{b_G}$ with $b_G = 0.0092 \pm 0.0073$ [14]. It is in evident contradiction with the number, obtained previously from the NLO combined analysis of the data from HERA and the CERN SPS [15], namely $b_G = -0.267 \pm 0.043$ at $Q_0^2 = 9\ \mathrm{GeV}^2$. Taking into account new CCFR model-independent extractions of F_2 [4], it seems worth while to perform more careful studies of the preliminary CHORUS results. Moreover, it is rather interesting to try to verify from the CHORUS data the experimental behaviour of $\Delta x F_3$, found in Ref. [4].

It should be stressed that the CHORUS experiment has an attractive feature. Indeed, as can be clearly seen from Fig.1, it provides information about νN

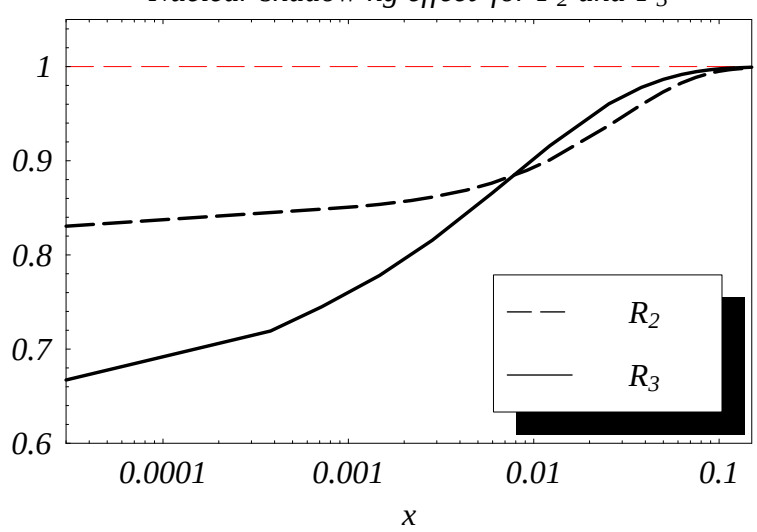

Figure 2: *The ratios of a heavy target to the free nucleon SFs* $R_2 = F_2^A/F_2^N$ *and* $R_3 = F_3^A/F_3^N$ *calculated for* ^{56}Fe *nucleus in the region of small* x *and* $Q^2 = 10$ GeV^2. *(the figure of Kulagin from Ref.* [10]*)*

DIS SFs in the region of rather low Q^2 and low x, which complement in part the one where the CCFR'97 data were extracted. In this kinematical domain, theoretical contributions of $1/Q^2$ and nuclear corrections can play an important role. Leaving for a while the discussions of power-suppressed terms, we stress that the CHORUS collaboration was using a lead target, while the CCFR target is made of iron. Possibilities are therefore really open to study nuclear effects in neutrino DIS; as shown in calculations reported in Ref. [16], these effects can be of great importance. A comparison of these effects for the cases of F_2 and xF_3 neutrino DIS SFs is depicted in Fig. 2, constructed for the detailed work of Ref. [10].

Another interesting possibility of DIS experiments is the extraction, from their chraracteristics, of non-perturbative power-suppressed terms and the values of $\alpha_s(M_Z)$. This question was considered in Refs. [17]– [23] in the process of the next-to-next-to-leading order (NNLO) QCD fits to different data, and in Ref. [24], while performing NLO fits to the experimental results for charged-leptons DIS SFs. The most recent outcomes of the NNLO analysis of the CCFR'97 xF_3 data [23] will be discussed in the next section. Here it is worth while emphasizing that the works of Refs. [17]– [20] [22] [23] agree in their conclusion that the inclusion of the NNLO QCD corrections into the fits has a tendency to decrease the extracted values of non-perturbative $1/Q^2$-terms. Whether this is a general theoretical feature (see e.g. Refs. [25] [26]) or it is related to the lack of precision of the analysed data might be clarified in the future, if the ideas of more detailed experiments on neutrino DIS at neutrino factories [10] are realized.

It should be noted that the situation at NLO is more transparent. Indeed, the Jacobi polynomial fits of Refs. [17] [19] [23] demonstrated that it is then pos-

Table 1: *The results of the fit, in Ref.* [5], *of the IRR model to the data from different neutrino experiments. The value of* χ^2 *over the number of points (np) is given.*

Experiment	Λ_3^2[GeV^2]	χ^2/np
IHEP–JINR	0.69 ± 0.37	3/12
CCFR'97	0.36 ± 0.22	253/222

sible to determine both $1/Q^2$ twist-4 effects and $\alpha_s(M_Z)$ from the CCFR'97 xF_3 experimental results, cut at $Q^2 \geq 5$ GeV^2. Moreover, the NLO DGLAP fits of Ref. [14] confirmed this feature, using both xF_3 and a cut at $x > 0.1$ on F_2 νN CCFR'97 data. A similar conclusion was made in the process of NLO DGLAP fits of intermediate-energy charged leptons data [24]. However, it is obvious that it is simpler to detect non-perturbative effects in a smaller Q^2-region.

The most recent example of such a determination was given by the NLO DGLAP analysis [5] of DIS neutrino data from JINR–IHEP Neutrino Detector collaboration, which collected rather large statistics (5987 neutrino and 741 antineutrino charged-current events) in a rather low-energy region 0.55 GeV^2 $\leq Q^2 \leq$ 20 GeV^2. The non-perturbative $1/Q^2$ correction to the perturbation theory (PT) behaviour of xF_3 was parametrized using the infrared renormalon (IRR) model of Ref. [27], namely

$$xF_3(x,Q^2) = xF_3^{PT}(x,Q^2) + \frac{h(x)}{Q^2} \quad , \tag{1}$$

where

$$h(x) = A_2^{'} \int_x^1 \frac{dz}{z} C_3^{IRR}(z) p_{NS}(x/z, Q^2) \quad , \tag{2}$$

C_3^{IRR} is the IRR model coefficient function, $xp_{NS}(x,Q_0^2) = Ax^{b_{NS}}(1-x)^{c_{NS}}$ is the boundary parton distribution, defined at $Q_0^2 = 0.5$ GeV^2 at NLO, and $A_2^{'}$ is the normalization parameter, which should be determined from the fits. It is sometimes expressed through the parameter Λ_3 as

$$A_2^{'} = -\frac{2C_F}{\beta_0}\Lambda_3^2 \quad , \tag{3}$$

where $C_F = 4/3$ and $\beta_0 = (11 - 2/3f)$ is the first coefficient of the QCD β-function. Fixing $\alpha_s(M_Z) = 0.118$, which corresponds to its world-average value, Λ_3 was extracted from the fits to the IHEP–JINR Neutrino Dectector and CCFR'97 data [5]. The results are presented in Table 1, taken from Ref. [5]. Note that the two expressions for Λ_3^2 from Table 1 are comparable within the errors. Averaging the numbers for Λ_3^2 and transforming them to $A_2^{'}$, the authors of Ref. [5] obtained the following value:

$$A_2^{'} = -0.130 \pm 0.056 \text{ (exp)} \ \text{ GeV}^2 \quad , \tag{4}$$

where the error includes both statistical and systematic experimental uncertainties. It is in agreement with the value extracted from the NLO Jacobi polynomial analysis of the CCFR'97 xF_3 behaviour, cut at $Q^2 \geq 5$ GeV^2 [17) 19) 23)]. Indeed, at NLO, the most detailed fits of Ref. [23)] give :

$$A_2^{'} = -0.125 \pm 0.053 \quad \text{(stat)} \quad \text{GeV}^2 \quad . \tag{5}$$

Note, however, that the error in Eq.(5) does not include the systematic uncertainties. Therefore, Eq.(4) is the most precise up-to-date value of the IRR model parameter $A_2^{'}$.

3 New QCD fits to CCFR xF_3 data: NNLO and beyond

We can start the discussion on the phenomenological application of some new N^{3}LO perturbative QCD results on the coefficient functions of odd moments of xF_3 and on the NNLO approximations for the related anomalous dimensions [28)] (which are complementary to those obtained in Ref. [29)] in the case of even moments for the F_2 SF of charged-leptons DIS), in combination with the NNLO expressions for the coefficient functions [30)] that were recently confirmed in Ref. [31)].

3.1 The application of the Jacobi polynomial method

It is appropriate, at this point to recall the basic ideas of the Jacobi polynomial method [32)] which was developed in Refs. [33) 34)] and was previously used in the analysis of the BCDMS charged-leptons DIS data at NLO [35)], and in the non-singlet approximation at NNLO [36)]. In the case of the analysis of the CCFR xF_3 data, the Jacobi polynomial method was applied at NLO in Refs. [37) 38)] and proved useful for performing fits at the NNLO [17) 19) 23)] and approximate N^{3}LO levels, [19) 23)] with and without twist-4 corrections (see discussion below).

This method allows the reconstruction of the SF (say xF_3) from the **finite** number of Mellin moments, namely

$$xF_3^{N_{max}}(x,Q^2) = x^\alpha (1-x)^\beta \sum_{n=0}^{N_{max}} \Theta_n^{\alpha\beta}(x) \sum_{j=0}^{n} c_j^{(n)}(\alpha,\beta) M_{j+2,F_3}^{TMC}(Q^2) + \frac{h(x)}{Q^2} \quad , \tag{6}$$

where $\Theta_n^{\alpha,\beta}$ are the Jacobi orthogonal polynomials with parameters α, β; $c_j^{(n)}(\alpha,\beta)$ is the combination of Euler Γ-functions. It increases factorially with increasing n. The Mellin moments M_{n,F_3}^{TMC} include information on the $1/Q^2$ target mass corrections and are defined as

$$M_{n,F_3}^{TMC}(Q^2) = \int_0^1 x^{n-1} F_3^{PT}(x,Q^2) dx + \frac{n(n+1)}{n+2} \frac{M_{nucl}^2}{Q^2} M_{n+2,F_3}(Q^2) \quad . \tag{7}$$

Table 2: *The NNLO results of the parameters A, b, c of the model for xF_3 determined, in Ref. [23] and their comparison with the values obtained in Ref. [40]. The new ones are marked by bold type.*

Order/N_{max}	Q_0^2	A	b	c	χ^2/np
NNLO/6	5 GeV^2	4.25±0.38	0.66±0.03	3.56±0.07	78.4/86
NNLO/9		**3.73±0.68**	**0.63±0.05**	**3.52±0.08**	**72.4/86**
NNLO /6	10 GeV^2	4.50±0.36	0.65±0.03	3.73±0.07	76.3/86
NNLO/9		**4.21±0.35**	**0.63±0.03**	**3.73±0.07**	**74.2/86**
NNLO/6	20 GeV^2	4.70±0.34	0.65±0.03	3.88±0.08	77.0/86
NNLO/9		**4.49±0.25**	**0.63±0.02**	**3.89±0.06**	**75.8/86**
NNLO/6	100 GeV^2	4.91±0.28	0.63±0.02	4.11±0.10	80.0/86
NNLO/9		**4.74±0.32**	**0.61±0.02**	**4.14±0.09**	**77.8/86**

The contribution of the twist-4 terms to Eq.(6) is parametrized with the help of the function $h(x)$. It will be neglected for our first stage of discussions.

Fixing now the behaviour xF_3 at the initial scale Q_0^2 as

$$xF_3^{PT}(x,Q_0^2) = A(Q_0^2)x^{b(Q_0^2)}(1-x)^{c(Q_0^2)}(1+\gamma(Q_0^2)) \quad , \tag{8}$$

calculating the related Mellin moments and transforming them to experimentally accessible regions with the help of the renormalization group technique at LO, NLO, NNLO and approximate N^{3}LO (the explicit formulae for the renormalization group evolution can be found in Ref. [23]), substituting the renormalization-group-improved expression for $M_{n,F_3}^{TMC}(Q^2)$ into Eq. (6), and performing the fits to the experimental data, it is possible to determine 5 parameters, namely A, b, c, γ and $\Lambda^{(4)}_{\overline{MS}}$; this enters the QCD coupling constant α_s, defined up to N^{3}LO, by means of the solution of the renormalization group equation for the explicitly known 4-loop approximation of the QCD β-function [39]. In Table 2 the new NNLO results of Ref. [23] for the parameters A, b, c of the model of Eq.(8) are presented. One can notice that, although these results agree with those of Ref. [40] within the statistical errors, the central values of the new numbers are over 0.03 lower, and the new fits have smaller values of χ^2.

It should be stressed that the new multiloop calculations of Ref. [28] allow us to use more moments in Eq. (6), namely $n = 13$, which corresponds to fixing $N_{max} = 9$. All this information was effectively used in Ref. [23]. Note that the previous, similar xF_3 fits of Refs. [17] [19] were made in the case of $n = 10$ and $N_{max} = 6$; they were using the approximate NNLO expressions for non-singlet anomalous dimensions, obtained from exact NNLO expressions for the anomalous dimensions of even non-singlet moments of F_2, calculated in Ref. [29]. Thus the considerations of Ref. [23] contain less uncertainties than the previous analysis of Refs. [17] [19]. The NNLO and N^{3}LO results for $\Lambda^{(4)}_{\overline{MS}}$, obtained in Ref. [23] in the process of twist-4

Table 3: *The Q_0^2 and N_{max} dependence of $\Lambda^{(4)}_{\overline{MS}}$ (in MeV) from Ref. [23]. The values of χ^2 are presented in parenthesis.*

N_{max}	Q_0^2 (GeV^2)	5	8	10	20	50	100
6	NNLO	297±30	314±34	320±34	327±36	327±35	326±35
		(77.9)	(76.3)	(76.2)	(76.9)	(78.5)	(79.5)
7	NNLO	326±34	327±35	327±35	326±36	327±36	328±35
		(75.9)	(76.7)	(77.1)	(78.1)	(78.8)	(78.7)
8	NNLO	334±35	334±35	333±35	331±35	328±35	328±35
		(74.3)	(75.7)	(76.2)	(77.4)	(78.3)	(78.5)
9	NNLO	330±33	332±35	333±34	331±37	330±35	329±35
		(72.4)	(73.6)	(74.7)	(75.8)	(76.7)	(77.8)
6	N^{3}LO	303±29	317±31	321±32	325±33	325± 33	324±33
		(76.4)	(75.6)	(75.7)	(76.6)	(78.0)	(78.7)
7	N^{3}LO	328±32	326±33	325±33	322±33	324± 33	324±33
		(76.2)	(77.0)	(77.3)	(78.2)	(78.5)	(78.2)
8	N^{3}LO	334±33	329±33	327±34	324±34	323± 34	324±34
		(74.8)	(76.2)	(76.6)	(77.4)	(77.3)	(77.2)
9	N^{3}LO	330±31	329±34	329±32	325±33	325± 32	325±33
		(73.3)	(74.6)	(75.7)	(76.4)	(76.7)	(76.8)

independent fits, are presented in Table 3. One can see that the application of new information from Ref. [28], which allowed N_{max} in Eq. (6) to go from 6 to 9, leads to better stability of $\Lambda^{(4)}_{\overline{MS}}$ with respect to changes of the initial scale Q_0^2, and decreases the values of χ^2.

It is interesting to compare the NNLO results for $b(Q_0^2)$ from Table 2 , which are almost Q_0^2-independent, with the calculations of the small-x asymptotic behaviour of non-singlet contributions to F_1 and the spin-dependent SF g_1 performed in Ref. [41] in all orders of 1-loop expression for α_s, using in part the approach developed in Ref. [42]. In the process of calculations of Ref. [41] the following 1-loop formula for α_s was used

$$\begin{aligned} \alpha_s(s) &= \frac{4\pi}{\beta_0 \ln(-s/\Lambda^2)} = \frac{4\pi}{\beta_0[ln(s/\Lambda^2) - i\pi]} \\ &= \frac{4\pi}{\beta_0}\Big[\frac{\ln(s/\Lambda^2)}{\ln^2(s/\Lambda^2)+\pi^2} + \frac{i\pi}{\ln^2(s/\Lambda^2)+\pi^2}\Big] \ , \end{aligned} \tag{9}$$

where $\Lambda = \Lambda^{(f=3)} = 0.1$. Note that the idea of taking into account the effects of π^2-terms in the perturbative expansion parameter is not new. It was previously used in a number of works on the subject [43]– [46] (for recent applications see in particular Ref. [47] and Ref. [48] where other related works were discussed as well).

The solution of the corresponding equations, which will not be presented

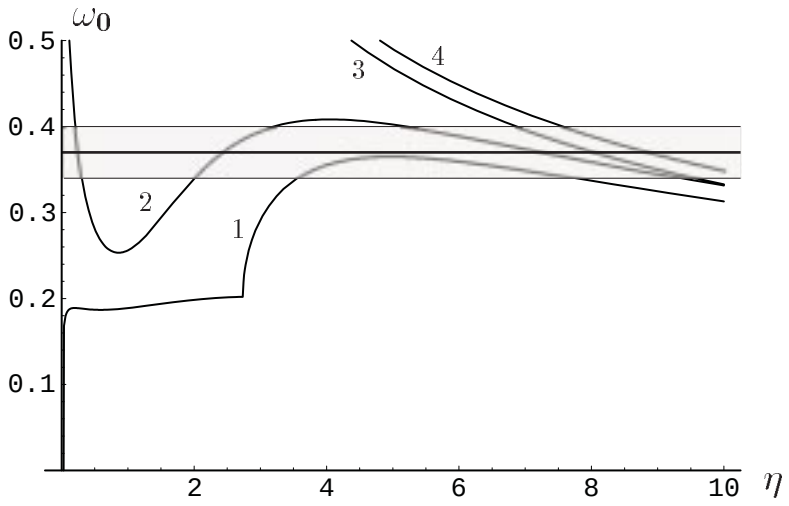

Figure 3: *Dependence of* ω_0 *on* $\eta = \ln(\mu^2/\Lambda^2)$. *1: for* F_1^{NS}, *2: for* g_1^{NS}, *3 and 4: for* F_1^{NS} *and* g_1^{NS}, *respectively, without accounting for the* π^2*-terms (from Ref.* [41]). *The results of the fits of Ref.* [23] *are added.*

here, and the application of Eq. (9) allowed the authors of Ref. [41] to obtain the following small-x asymptotic behaviour of F_1^{NS} and g_1^{NS} :

$$\begin{aligned} F_1^{NS} &\sim \left(\frac{1}{x}\right)^{\omega_0^{(+)}} \left(\frac{Q^2}{\mu^2}\right)^{\omega_0^{(+)}/2} \\ g_1^{NS} &\sim \left(\frac{1}{x}\right)^{\omega_0^{(-)}} \left(\frac{Q^2}{\mu^2}\right)^{\omega_0^{(-)}/2} \end{aligned} \qquad (10)$$

,

where the powers $\omega_0^{(+)}$ and $\omega_0^{(-)}$ are drawn in Fig. 3, taken from Ref. [41]. This plot is supplemented with the bounds on the values of $\omega_0 = 1 - b(Q_0^2)$, which come from the results presented in Table 2 and obtained in the process of the fits to the CCFR'97 data for the non-singlet SF xF_3, performed in Ref. [23] for $Q_0^2 \geq 5$ GeV^2. These values are lying in the area limited by straight lines, with the centre at $\omega_0 = 0.37$ shown in Fig. 3. It is worth trying to understand in more detail the possible relations between the results of Ref. [41] and those of Ref. [23]. Note, in particular, that the comparison seems to be more legitimate in the region $\eta \geq 8$, namely for $Q^2 > \mu^2 = 30$ GeV^2, than for low values of η, where the π^2-effects are playing the dominant role. This region is not considerably affected even by the transformation from $\Lambda^{(3)} \approx 0.1$ GeV, used in Ref. [41], to $\Lambda^{(3)} \approx 0.4$ GeV, which follows from the Q_0^2-independent numbers of Table 3, obtained when N_{max} is fixed to 9 in Eq. (6).

Consider now some other results of the work of Ref. [23], and in particular the extraction of twist-4 contributions and the value of $\alpha_s(M_Z)$ at various orders of perturbation theory. To model the $1/Q^2$-term $h(x)$ in Eq. (6), three approaches were used in Ref. [23]. The first one is the IRR model of Ref. [27] (see Eq. (2)).

After taking the Mellin moments from Eq. (2) and applying the NNLO and N^{3}LO fits to the CCFR'97 xF_3 data, the reductions of the NLO value of $A_2^{'}$, presented in Eq. (5), were observed. At the NNLO and N^{3}LO the expressions for $A_2^{'}$ become comparable with zero, within the statistical errors [23], namely

$$\begin{aligned} \text{NNLO} \quad &: \quad A_2^{'} \;=\; -0.013 \pm 0.051 \;\; \text{GeV}^2 \\ \text{N}^3\text{LO} \quad &: \quad A_2^{'} \;=\; 0.038 \pm 0.051 \;\; \text{GeV}^2 \quad . \end{aligned} \tag{11}$$

However, the related $\alpha_s(M_Z)$ results were determined in Ref. [23] with reasonable errors:

$$\begin{aligned} \text{NLO} \quad &: \quad \alpha_s(M_Z) \;=\; 0.1194 \pm 0.0022 \;\text{(stat)} \;\pm 0.005 \;\text{(syst)} \\ &\qquad\qquad \pm 0.0018 \;\text{(thresh)}^{+0.0096}_{-0.0063} \;\text{(scale)} \\ \text{NNLO} \quad &: \quad \alpha_s(M_Z) \;=\; 0.1188 \pm 0.0022 \;\text{(stat)} \;\pm 0.005 \;\text{(syst)} \\ &\qquad\qquad \pm 0.0017 \;\text{(thresh)}^{+0.0038}_{-0.0008} \;\text{(scale)} \\ \text{N}^3\text{LO} \quad &: \quad \alpha_s(M_Z) \;=\; 0.1188 \pm 0.0022 \;\text{(stat)} \;\pm 0.005 \;\text{(syst)} \\ &\qquad\qquad \pm 0.0017 \;\text{(thresh)}^{+0.0017}_{-0.0007} \;\text{(scale)} \end{aligned} \tag{12}$$

where the first theoretical uncertainty is due to the ambiguities of taking into account threshold effects while transforming the results for $\Lambda^{(5)}_{\overline{\text{MS}}}$ to a world with $f = 5$ numbers of active flavours (for a detailed explanation of how this uncertainty was fixed using the matching conditions of Ref. [49], see Ref. [23] and references therein) and the scale-dependence uncertainty was determined by choosing the factorization and renormalization scales $\mu_F^2 = \mu_R^2 = \mu^2_{\overline{MS}}\; k$ and varying k in the conventional interval $1/4 \leq k \leq 4$. One can notice the drastic reduction of the scale-dependence uncertainties as a result of adding NNLO and N^{3}LO perturbative QCD corrections into the fits, tabulated in the case of $f = 4$ in Ref. [23] (note that at the N^{3}LO the contributions to expanded anomalous-dimension terms were modelled using [1/1] Padé approximants).

The results for $\alpha_s(M_Z)$, presented in Eq. (12), should be compared with the ones obtained from the twist-4 independent Jacobi polynomial fits to the CCFR'97 data at $N_{max} = 9$ [23], which give

$$\begin{aligned} \text{NLO} \quad &: \quad \alpha_s(M_Z) \;=\; 0.1177 \pm 0.0024(\text{stat}) \pm 0.005(\text{syst}) \\ &\qquad\qquad \pm 0.00177(\text{thresh})^{+0.0070}_{-0.0047}(\text{scale}) \\ \text{NNLO} \quad &: \quad \alpha_s(M_Z) \;=\; 0.1188 \pm 0.0022(\text{stat}) \pm 0.005(\text{syst}) \\ &\qquad\qquad \pm 0.0017(\text{thresh})^{+0.0027}_{-0.0022}(\text{scale}) \\ \text{N}^3\text{LO} \quad &: \quad \alpha_s(M_Z) \;=\; 0.1184 \pm 0.0022(\text{stat}) \pm 0.005(\text{syst}) \\ &\qquad\qquad \pm 0.0017(\text{thresh})^{+0.0017}_{-0.0009}(\text{scale}) \end{aligned} \tag{13}$$

Notice that the effective minimization of the twist-4 contributions at the NNLO and N^{3}LO (see Eq. (11)) is leading to rather closed NNLO and N^{3}LO values of $\alpha_s(M_Z)$, which were obtained from the fits with and without $1/Q^2$ corrections.

It is worth stressing that errors on the scale dependence of the NLO and NNLO results from Eq. (13) have definite support. Indeed, they are in agreement with the independent estimates

$$\Delta\alpha_s(M_Z)_{NLO} =^{+0.006}_{-0.004} \quad , \quad \Delta\alpha_s(M_Z)_{NNLO} =^{+0.0025}_{-0.0015} \quad , \tag{14}$$

obtained in Ref. [50], which use the model constructed in this work for the NNLO NS DGLAP kernel.

In order to study the second possibility of modelling $1/Q^2$-effects using the parametrization of $h(x)$ by free constants $h_i = h(x_i)$, where x_i are the points in the experimental data binning, 9 parameters h_i were used in Ref. [23]. This choice distinguishes new fits from the ones performed in Refs. [17] [19], where 16 variables h_i were used. The minimization of the number of free parameters was motivated by the works of Refs. [24] [14], where it was demonstrated that a decrease in the number of fitted high-twist parameters decreases the correlation between their errors and make their extraction more reliable (the problems of estimating theoretical uncertainties in the case of the choice of 16 free parameters h_i were also discussed in Ref. [51]). The choice of a smaller number of h_i results in a more reliable description of the x-shape of $h(x)$ for the fits to the CCFR xF_3 data. As in the process of the analogous fits of Refs. [17] [19], the LO and NLO x-shapes of $h(x)$ obtained in Ref. [23] are in agreement with the prediction of the IRR model of Ref. [27]. The new NNLO and N^{3}LO results of Ref. [23], in agreement with the above-discussed tendency to an overall minimization of the extracted contribution of $h(x)$, reveal some new feature, namely an indication of an oscillating-type behaviour of $h(x)$ around $x = 0$, albeit with rather small amplitude.

The third model of $1/Q^2$-corrections, considered in Ref. [23], is directly expressed in terms of Mellin moments, namely

$$M_n^{HT}(Q^2) = n\frac{B_2'}{Q^2}M_n^{F_3}(Q^2) \tag{15}$$

with the free parameter B_2'. It is identical to the model used in Ref. [21] for fixing theoretical uncertainties of the extraction of $\alpha_s(M_Z)$ at NNLO with the help of the Bernstein polynomial technique, which will be discussed below.

In Ref. [23] it was shown that the precision of the CCFR'97 xF_3 data allows a determination of the value of B_2' together with $\alpha_s(M_Z)$ both at LO and NLO. However, as in the cases of the previous two models for $1/Q^2$-corrections, considered in Ref. [23], NNLO perturbative QCD effects screen the contribution of non-perturbative $1/Q^2$-corrections, defined through Eq. (15). It should be recalled,

in these circumstances, that the QCD fits of Ref. [52] to BEBC–Gargamelle [53] and CDHS [54] neutrino DIS data, performed over 20 years ago, did not allow a discrimination between $1/Q^2$ and the logarithmic description of scaling violation to be made. Therefore, it is possible to conclude that present neutrino DIS data now have become more precise. Indeed, their analysis shifted the effect of perturbative screening of $1/Q^2$-corrections from LO to NNLO. The next generation of more detailed tests of QCD in neutrino DIS is now on the agenda [10].

3.2 The application of the Bernstein polynomial method

In this part of our mini-review the basic steps of the Bernstein polynomial approach, proposed in Ref. [55] and recently used in the process of NNLO fits to the CCFR'97 xF_3 data in Ref. [21], will be recalled. The basic constructions of this approach are the Bernstein averages for the xF_3 SF :

$$F_{nk}^{F_3}(Q^2) = \int_0^1 dx p_{nk}(x) x F_3(x, Q^2) \quad , \tag{16}$$

where $p_{nk}(x)$ are the Bernstein polynomials, which can be presented, when $k \leq n$, in the following form:

$$p_{nk}(x) = p(n,k) \sum_{l=0}^{n-k} \frac{(-1)^l}{l!(n-k-l)!} x^{2(k+l)+1} \quad , \tag{17}$$

where $p(n,k)$ is defined as (see e.g. [21]):

$$p(n,k) = \frac{2(n-k)!\Gamma(n+\frac{3}{2})}{\Gamma(k+\frac{1}{2})\Gamma(n-k+1)} \quad . \tag{18}$$

Using Eqs. (16)–(18), it is possible to express the Bernstein averages for xF_3 through xF_3 odd Mellin moments as:

$$F_{nk}^{F_3}(Q^2) = p(n,k) \sum_{l=0}^{n-k} \frac{(-1)^l}{l!(n-k-l)!} M_{(2k+2l+1),F_3}(Q^2) \quad . \tag{19}$$

The next step is similar to the one used in the process of applications of the Jacobi polynomial technique. At some initial scale Q_0^2, xF_3 can be parametrized through Eq.(8), several odd Mellin moments of xF_3 at Q_0^2 defined and then transformed using NNLO renormalization group equations at the appropriate values of Q^2, which enter into the kinematical region of the analysed experimental data. Forming now Bernstein averages of Eq. (18) it is possible to fit them to their experimental values. In the case of the CCFR'97 xF_3 data, fits were made in the kinematical region 7.9 GeV$^2 \leq Q^2 \leq$ 125.9 GeV^2 [21]. The following numbers for $\alpha_s(M_Z)$ were obtained [21] from these fits :

$$\begin{aligned} \text{NLO} \quad &: \quad \alpha_s(M_Z) \;=\; 0.116 \pm 0.004 \text{ (exp)} \\ \text{NNLO} \quad &: \quad \alpha_s(M_Z) \;=\; 0.1153 \pm 0.004 \text{ (exp)} \quad , \end{aligned} \tag{20}$$

The final NNLO expression, which includes the estimates of some theoretical uncertainties, is [21]:

$$\text{NNLO} \quad : \qquad \alpha_s(M_Z) = 0.1153 \pm 0.0041 \ (\text{exp}) \pm 0.0061 \ (\text{theor}) \quad , \qquad (21)$$

It is worth while to mention that, despite the qualitative agreement, the central NLO values of Eq.(20), obtained with the help of the Bernstein polynomial technique, are lower than the existing determinations of $\alpha_s(M_Z)$ from the CCFR'97 xF_3 data, which result from the NLO DGLAP analysis [3] [14] and the application of the Jacobi polynomial technique [17] [19] [23]. Moreover, at NNLO, the result of Eq. (21) intersects with the NNLO determination of $\alpha_s(M_Z)$ of Ref. [23] (see Eqs.(12) and (13)) within existing errors only. The comparison between the results of the Jacobi and Bernstein polynomial determinations of $\alpha_s(M_Z)$ and of the related theoretical uncertainties was presented in Ref. [23]. In the process of these studies, definite disagreements were revealed between some results of the works of Ref. [21] and Ref. [23]. The origin of these disagreements is unclear at present and stimulates a more detailed analysis of the NNLO realizations of the Jacobi and Bernstein polynomial approaches. Note, however, that the definite choice of the scale parameter in the Jacobi polynomial fits leads to improving the agreement of the results of applications of the two methods [23]. In view of this observation, it is possible that the results of Ref. [21] contain larger theoretical uncertainties due to the neglect of scale-dependence ambiguities. On the other hand, contrary to the Bernstein polynomial analysis, the NNLO Jacobi polynomial fits of Ref. [23] also used approximate information about the values of the NNLO corrections to anomalous dimensions of even moments of xF_3. It should be stressed that this approximation can be eliminated after completing the program of explicit calculations of NNLO contributions to non-singlet DGLAP kernels, which is now in progress [56]. As to the current applications of the DGLAP method in the concrete NNLO fits to DIS data, they can in principle be based on the machinery of the Bayesian treatment of systematic errors of DIS data (see e.g. Ref. [15]) and the approximate NNLO models of DGLAP kernels, constructed in Refs. [50] [57] [58].

Acknowledgements

I am grateful to G. Parente and A. V. Sidorov for our long and fruitful collaboration, which led us to a number of inspiring (at least for me) results discussed in this mini-review and to A. V. Kotikov for his contribution to our common works. It is a pleasure to thank S.I. Alekhin, G. Altarelli, S. Catani, B.I. Ermolaev, S.A. Kulagin and F. J. Yndurain for many useful discussions. It is an honour to express my warm gratitude to J. Tran Thanh Van, who contributed a lot to organizing non-formal discussions between experimentalists and theoreticians during the Rencontres de Moriond QCD sessions, which had an essential influence on the works discussed above, and especially on those devoted to the study of neutrino DIS data of the CCFR collaboration. Special thanks go to M. Greco for giving me the possibility to present the talk at the very productive La Thuile Conference. I also would like to express my special thanks to the members of the Theoretical Physics Division of CERN for creating such a pleasant scientific atmosphere.

References

1. J. M. Conrad, M. H. Shaevitz and T. Bolton, Rev. Mod. Phys. **70**, 1341 (1998).

2. A. L. Kataev and A. V. Sidorov, The Gross– Llewellyn Smith sum rule: Theory versus experiment, CERN-TH/7235-94 [hep-ph/9405254]; in Proc. 29th Rencontres de Moriond "94 QCD and High Energy Hadronic Interactions", ed. J. Tran Thanh Van, Méribel, 1994, (Editions Frontières, 1994) 189.

3. W. G. Seligman *et al.*, Phys. Rev. Lett. **79**, 1213 (1997) .

4. U. K. Yang *et al.*, Phys. Rev. Lett. **86**, 2742 (2001) .

5. S. I. Alekhin *et al.* [IHEP-JINR Neutrino Detector Collaboration], Phys. Lett. **B512**, 25 (2001) [hep-ex/0104013] .

6. R. G. Oldeman [CHORUS Collaboration], Status of the CHORUS structure function measurement, in Proc. 7th Int. Workshop DIS99, Zeuthen, April 1999 eds. J. Blumlein and T. Riemann, Nucl. Phys. Proc. Suppl. **B79**, 96 (1999) .

7. R. G. Oldeman [CHORUS Collaboration], Measurement of differential neutrino-nucleon cross-sections and structure functions using the CHORUS lead calorimeter, talk at ICHEP 2000 Conference, Osaka; to be published in the Proceedings (World Scientific, in press).

8. U. Bassler, E. Laenen, A. Quadt and H. Schellman, in Proc. 7th Int. Workshop DIS99, Zeuthen, 1999, eds. J. Blumlein and T. Riemann, Nucl. Phys. Proc. Suppl. **B79**, 701 (1999).

9. A. de Rujula, Neutrino physics at the Neutrino factory, talk at Int. Workshop NuFact'00, Monterey, California, USA, May 2000.

10. M. L. Mangano *et al.*, "Physics at the front-end of a neutrino factory: A quantitative appraisal," CERN-TH/2001-131 [hep-ph/0105155].

11. P. Amaudruz *et al.* [New Muon Collaboration], Nucl. Phys. **B441**, 3 (1995) .

12. S. Kretzer, F. I. Olness, R. J. Scalise, R. S. Thorne and U. K. Yang, Phys. Rev. **D64**, 033003 (2001) [hep-ph/0101088].

13. V. N. Gribov and L. N. Lipatov, Sov. J. Nucl. Phys. **15**, 438 (1972); L. N. Lipatov, Sov. J. Nucl. Phys. **20**, 94 (1975); G. Altarelli and G. Parisi, Nucl. Phys. **B126**, 298 (1977); Yu. L. Dokshitzer, Sov. Phys. JETP **46**, 641 (1977).

14. S. I. Alekhin and A. L. Kataev, Phys. Lett. **B452**, 402 (1999) [hep-ph/9812348].

15. S. Alekhin, Eur. Phys. J. **C10**, 395 (1999) [hep-ph/9611213].

16. S. A. Kulagin, Nuclear shadowing in neutrino deep inelastic scattering [hep-ph/9812532], in Proc. 14th Int. Seminar on Relativistic Nuclear Physics and Quantum Chromodynamics, Dubna, 1998, eds. A. M. Baldin et al.

17. A. L. Kataev, A. V. Kotikov, G. Parente and A. V. Sidorov, Phys. Lett. **B417** 374 (1998) [hep-ph/9706534]; presented in part at 32nd Rencontres de Moriond: QCD and High-Energy Hadronic Interactions, Les Arcs, 1997, ed. J. Tran Thanh Van (Editions Frontières, 1997), p. 335.

18. U. K. Yang and A. Bodek, Phys. Rev. Lett. **82**, 2467 (1999) [hep-ph/9809480].

19. A. L. Kataev, G. Parente and A. V. Sidorov, Nucl. Phys. **573**, 405 (2000).

20. A. D. Martin, R. G. Roberts, W. J. Stirling and R. S. Thorne, Eur. Phys. J. **C18**, 117 (2000) [hep-ph/0007099].

21. J. Santiago and F. J. Yndurain, FTUAM-01-01 [hep-ph/0102247].

22. S. Schaefer, A. Schafer and M. Stratmann, hep-ph/0105174.

23. A. L. Kataev, G. Parente and A. V. Sidorov, CERN-TH/2001-58, hep-ph/0106221.

24. S. I. Alekhin, Phys. Rev. **D59** 114016 (1999) [hep-ph/9809544]; Combined analysis of SLAC-BCDMS-NMC data at high x: $\alpha(s)$ and 'high twists', hep-ph/9907350, in Proc. 34th Rencontres de Moriond: QCD and Hadronic Interactions, Les Arcs, 1999, ed. by J. Tran Thanh Van.

25. A. A. Penin and A. A. Pivovarov, Phys. Lett. B **B401**, 294 (1997).

26. Y. L. Dokshitzer, Perturbative QCD and power corrections, hep-ph/9911299; in Proc. 11th Rencontres de Blois: Frontiers of Matter, Blois, 1999, ed. J. Tran Thanh Van.

27. M. Dasgupta and B. R. Webber, Phys. Lett. **B382**, 273 (1996).

28. A. Retey and J. A. Vermaseren, Nucl. Phys. **B604**, 281 (2001) [hep-ph/0007294].

29. S. A. Larin, T. van Ritbergen and J. A. Vermaseren, Nucl. Phys. **B427**, 41 (1994); S. A. Larin, P. Nogueira, T. van Ritbergen and J. A. Vermaseren, Nucl. Phys. **B492**, 338 (1997) [hep-ph/9605317].

30. E. B. Zijlstra and W. L. van Neerven, Phys. Lett. **B297**, 377 (1992).

31. S. Moch and J. A. Vermaseren, Nucl. Phys. **B573**, 853 (2000).

32. G. Parisi and N. Sourlas, Nucl. Phys. **B151**, 421 (1979).

33. J. Chyla and J. Rames, Z. Phys. **C31**, 151 (1986).

34. V. G. Krivokhizhin *et al.*, Z. Phys. **C36**, 51 (1987) and **C48**, 347 (1990).

35. A. C. Benvenuti *et al.* [BCDMS Collaboration], Phys. Lett. **B195**, 97 (1987) and **B223**, 490 (1989)

36. G. Parente, A. V. Kotikov and V. G. Krivokhizhin, Phys. Lett. **B333**, 190 (1994).

37. A. L. Kataev and A. V. Sidorov, Phys. Lett. **B331**, 179 (1994).

38. J. Chyla and J. Rames, Phys. Lett. **B343**, 351 (1995).

39. T. van Ritbergen, J. A. Vermaseren and S. A. Larin, Phys. Lett. **B400**, 379 (1997).

40. A. L. Kataev, G. Parente and A. V. Sidorov, Nucl. Phys. **A666-667**, 184 (2000).

41. B. I. Ermolaev, M. Greco and S. I. Troyan, Nucl. Phys. **B594**, 71 (2001).

42. R. Kirschner and L. N. Lipatov, Nucl. Phys. **B213**, 122 (1983).

43. A. V. Radyushkin, Preprint JINR-E2-82-159 (1982); JINR Rapid Commun. **78**, 96 (1996) [hep-ph/9907228].

44. N. V. Krasnikov and A. A. Pivovarov, Phys. Lett. **B116**, 168 (1982).

45. S. G. Gorishny, A. L. Kataev and S. A. Larin, Sov. J. Nucl. Phys. **40**, 320 (1984) [Yad. Fiz. **40**, 517 (1984)].

46. A. A. Pivovarov, Z. Phys. **C53**, 461 (1992).

47. D. V. Shirkov, Theor. Math. Phys. **127**, 409 (2001) [hep-ph/0012283].

48. D. J. Broadhurst, A. L. Kataev and C. J. Maxwell, Nucl. Phys. **B592**, 247 (2001).

49. K. G. Chetyrkin, B. A. Kniehl and M. Steinhauser, Phys. Rev. Lett. **79**, 2184 (1997).

50. W. L. van Neerven and A. Vogt, Nucl. Phys. **B568**, 263 (2000).

51. S. Forte, Recent developments in deep-inelastic scattering, hep-ph/9812382, Proc. La Thuile 1999; Results and perspectives in particle physics, ed. M. Greco, p. 377.

52. L. F. Abbott and R. M. Barnett, Ann. Phys. **125**, 276 (1980).

53. P. C. Bosetti *et al.*, Nucl. Phys. **B142**, 1 (1978).

54. J. G. de Groot *et al.*, Z. Phys. **C1**, 143 (1979).

55. F. J. Yndurain, Phys. Lett. **B74**, 68 (1978).

56. S. Moch and J. A. Vermaseren, work in progress (private communication).

57. W. L. van Neerven and A. Vogt, Nucl. Phys. **B588**, 345 (2000).

58. W. L. van Neerven and A. Vogt, Phys. Lett. **B490**, 111 (2000).